A Multi-Objective Simulated Annealing Approach to Reactive Power Compensation

Carlos H. Antunes, Paulo Lima, Eunice Oliveira, Dulce Pires

A Multi-Objective Simulated Annealing Approach to Reactive Power Compensation

Journal:	*Engineering Optimization*
Manuscript ID:	GENO-2010-0070.R3
Manuscript Type:	Original Article
Date Submitted by the Author:	04-Oct-2010
Complete List of Authors:	Antunes, Carlos; University of Coimbra, Dep. Electrical Engineering and Computers Lima, Paulo; INESC Coimbra Oliveira, Eunice; ESTG- IP Leiria Pires, Dulce; EST - IP Setúbal
Keywords:	Multi-objective optimization, Simulated annealing, Electrical distribution networks

A Multi-Objective Simulated Annealing Approach to Reactive Power Compensation

Carlos Henggeler Antunes* (1,4), Paulo Lima (4), Eunice Oliveira (3,4), Dulce F. Pires (3,4)

(1) Dept. of Electrical Engineering and Computers, University of Coimbra; Polo II, 3030 Coimbra, Portugal

(2) School of Technology and Management, Polytechnic Institute of Leiria; Morro do Lena, Ap. 4163, 3411-901 Leiria, Portugal

(3) School of Technology, Polytechnic Institute of Setúbal; 2910-761 Setúbal, Portugal

(4) R&D Unit INESC Coimbra; Rua Antero de Quental 199, 3030 Coimbra, Portugal

* Corresponding author. Email: ch@deec.uc.pt

Reactive power compensation is an important problem in electrical distribution systems, involving the sizing and location of capacitors (sources of reactive power). The installation of capacitors also contributes to releasing system capacity and improving voltage level. A multi-objective simulated annealing approach to provide decision support in this problem is presented. This approach is able to compute a set of well-distributed and diversified solutions underlying distinct trade-offs, even for a challenging network. The characterization of the non-dominated front is relevant information for aiding planning engineers to select satisfactory compromise solutions (compensation schemes) to improve the network operation conditions.

1. Introduction

The installation of shunt capacitors in electricity distribution networks is often necessary for the compensation of reactive power due to inductive loads. Those sources of reactive power are aimed at guaranteeing an efficient delivery of active power to loads, releasing electric system capacity, improving the bus voltage profile and reducing losses. The problem of reactive power compensation involves determining the network nodes and the size of the capacitors to be installed. The merit of the solutions (characterized by the location and size of capacitors) is evaluated according to economical, technical and quality of service objectives. These multiple, conflicting and incommensurate evaluation aspects must be explicitly incorporated (and not just combined into a questionable monetary function) into mathematical models for decision support, in order to identify the non-dominated frontier and grasping the compromises at stake between the competing objective functions. Therefore a multi-objective model has been

developed (Antunes *et al.* 2009) including cost and power losses as objective functions. The voltage profile has been considered as a set of constraints, according to technical and quality of service requirements. This offers planning engineers a broad view of the trade-offs between cost (economical dimension) and losses (technical dimension) that can be established in different regions of the search space where solutions with distinct characteristics can be computed.

Mathematical models for this problem require binary, integer and real-valued decision variables, also involving linear and nonlinear (associated with physical laws in networks) constraints. Due to these characteristics and the intrinsic combinatorial nature of this problem, meta-heuristic approaches have been revealed to be quite adequate for computing solutions and identifying the non-dominated (Pareto optimal) frontier.

The reactive power compensation problem has been studied in the last four decades. Algorithmic approaches to tackle the problem include mathematical programming techniques (generally requiring some less realistic assumptions on the network characteristics for the sake of computer tractability) and, more recently, meta-heuristics. Simulated Annealing, Ant Colony Optimization, Particle Swarm Optimization, Tabu Search and Evolutionary/Genetic Algorithms have been used to deal with this problem, considering both single and multi-objective models (Zhang *et al.* 2007). Meta-heuristics have indeed been shown to be quite adequate to cope with model complexity and tractability as well as to reduce the exhaustive search in large spaces by appropriately sampling the search space. Moreover, experiments with real-world challenging problems indicate that meta-heuristics with an adequate parameterization can lead to truly (or near) non-dominated solutions (Glover and Kochenberger, 2003).

The interest and motivation of the study have been provided in this Introduction. An overview of the multi-objective model for reactive power compensation in distribution networks is presented in section 2. An approach based on simulated annealing for characterizing the non-dominated front (costs vs. power losses) for the multi-objective model is presented in section 3. Results are presented in section 4, and some conclusions are drawn in section 5.

2. Overview of a multi-objective mathematical model

The reactive power compensation problem has been formulated as a non-linear mixed integer problem with two (conflicting and incommensurate) objective functions to be minimized: active power losses and investment costs. The main constraints include voltage limits at each bus, impossibility to locate capacitors in certain nodes, operational constraints due to the required load to supply at each node, and the power flow equations in the network (physical laws). A

solution consists in a compensation scheme, that is, the size of the capacitors to be located in each network node establishing a compromise between active power losses and costs, while satisfying the sets of constraints.

An example of a radial electrical distribution network is displayed in Figure 1. SE is the sub-station, from which power flows into the network. The nodes indicate the load demand points or derivations to lateral buses in which capacitors may be installed.

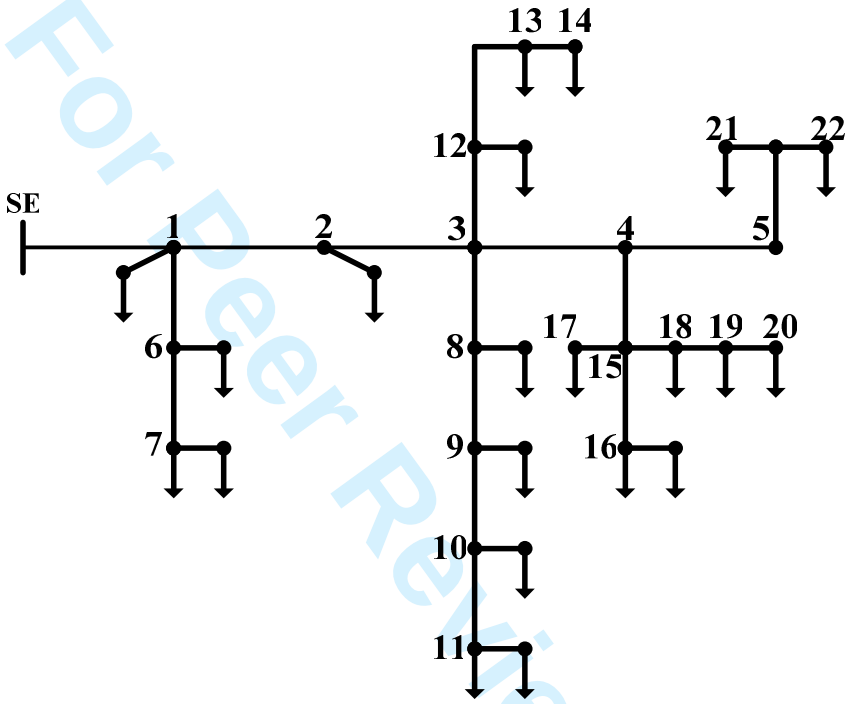

Fig. 1 - Example of a radial electrical distribution network

The connection between network buses is illustrated in Figure 2. Load and compensation devices (capacitors) are directly connected to bus *m*. which is fed by a preceding bus and supplies other subsequent buses (*j, j+1,…, j+n*). The connection branches are characterized by their resistance and reactance. The power flow algorithm computes the (active and reactive) power, as well as the voltage, at each network node resulting from a given compensation scheme, that is, a solution representing a given location and sizing of the capacitors. This iterative algorithm has been implemented with MATLAB using complex numbers to achieve more accurate results. It takes advantage of the radial structure of distribution networks to simplify the computation. For more technical details on the power flow algorithm, see Pires *et al.* (2009).

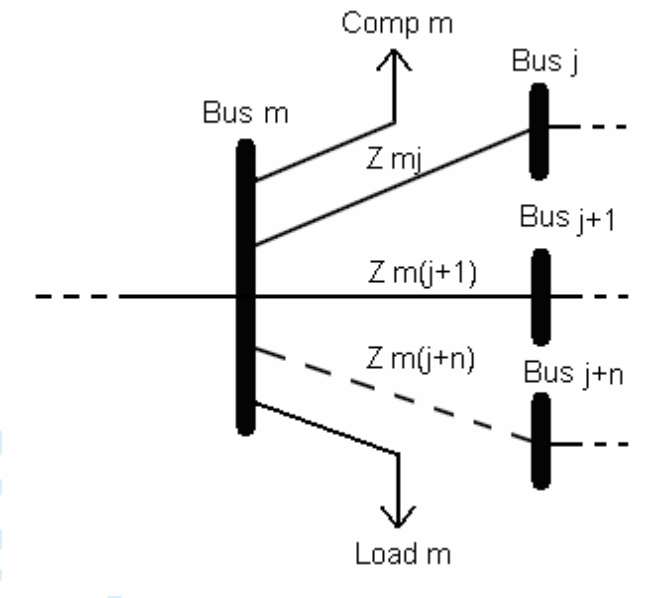

Fig. 2 - Connection between buses

The real-valued variables are the (active and reactive) power magnitudes flowing in the network and the node voltage. The integer decision variables encode the decision whether a new capacitor of a certain type is installed in a given node. New capacitors are characterized by their capacity and the acquisition cost. Standard units, generally used in distribution systems, are considered.

The multi-objective mathematical model is presented in Appendix A (see also Pires *et al.* 2009, for further details).

3. A Multi-Objective Simulated Annealing Approach

The multi-objective simulated annealing approach relies on the use of the non-dominance relation and it just uses some form of aggregation whenever the acceptance probability function is required to intervene. Three main processes may be distinguished: random generation of compensation solutions, generation of compensation solutions using different types of neighbourhood structures, and selection of non-dominated solutions. This particular application of the multi-objective simulated annealing approach to the case study in reactive power compensation includes an additional process concerning the analysis of the power flow in the radial electrical distribution network, which is responsible for assessing the feasibility of solutions.

Each solution (compensation scheme), generated either by a random location of capacitors or a move to a neighbour solution in the operational framework of the simulated annealing procedure, is analyzed for the satisfaction of the system operation (power flow) equations and

lower/upper bounds of voltage at the nodes (these resulting from quality of service aspects generally imposed by regulations). Only feasible solutions regarding to the sets of constraints are retained for further analysis.

The initial solutions are generated randomly, although other techniques could be envisaged such as distributing capacitors more or less regularly along the network. The random generation of solutions involves defining, within the range of capacity values and technically feasible nodes to install capacitors:

- the network nodes where a capacitor is installed;
- the capacity of the capacitors to install.

A routine for selecting the non-dominated solutions is called to build up the archive, thus consisting of non-dominated solutions only, for the simulated annealing procedure.

Solutions are encoded by a string of integers indexed by the network node (Figure 3): 0 means that no capacitor is installed in that node and non-zero values indicate the capacitor type installed therein.

0	0	2	7	···	0	5	0	3

Fig. 3 - Solution encoding

The procedure samples the neighbourhood of all solutions currently in the archive, evaluating new solutions derived from the current solution. New solutions are generated from the initial compensation schemes by defining feasible moves transforming a solution s into a solution $s' \in N(s)$, that is, within its neighbourhood. The solutions in $N(s)$ are the ones that can be obtained from s by one of the following operations:

- Relocating a capacitor (possibly changing its value) currently installed to an uncompensated node (Figure 4 (a)).
- Reducing the capacity of the capacitor installed in a given node to the immediate lower size (Figure 4 (b)).
- Increasing the capacity of the capacitor installed in a given node to the immediate upper size (Figure 4 (c)).
- Removing the capacitor installed in a given node (Figure 4 (d)).
- Installing a new capacitor in a currently uncompensated node (Figure 4 (e)).
- Relocating the capacitor installed in a given node to an adjacent node (Figure 4 (f-g)).

Besides these neighbourhood structures another possibility of exploring new regions of the search space is based on the composition of the current solution with another solution of the

archive using components of both in the spirit of the crossover operator in genetic algorithms (Figure 4 (h)).

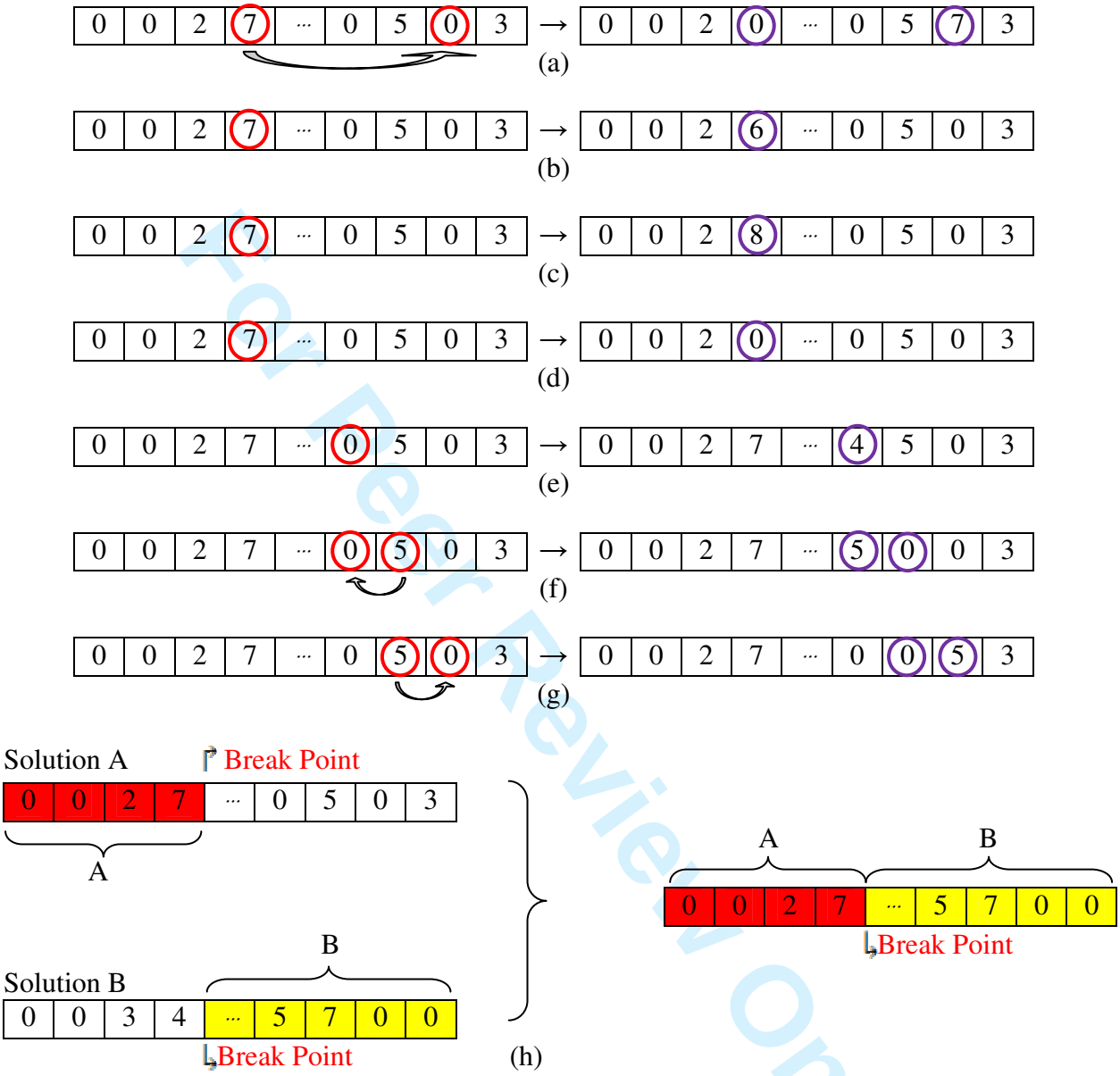

Fig. 4 – Examples of neighbourhood structures (8 different types of capacitors are considered)

Note that some of these operations (removing a capacitor or decreasing the capacity of a capacitor previously installed) guarantee the improvement of the cost objective function if the solution obtained remains a feasible one. However, the direction of the change of the active power losses objective function cannot be taken for granted, since it also depends on the capacitor location, load profile, etc. The change of the losses objective function can only be assessed after the power flow algorithm is executed for each configuration.

Those new solution construction strategies are used randomly and the corresponding rate of success is recorded in order to introduce a small bias for this process in the next temperature step. The aim is to endow the neighbourhood selection process with some adaptive features.

Temperature is decreased exponentially. For each value of temperature all the solutions in the archive are taken as the current solution and its neighbourhood is exploited. This exploitation (intensification phase) is performed involving the competition of a new solution (resulting from one of the neighbourhood strategies above) with the current solution (one in the current archive).

This competition may lead to different situations:

- If the new solution is dominated by the current solution, then the decision whether its neighbourhood is explored depends on the acceptance probability.
- If the new solution is neither dominated nor dominates the current solution as well as any other solution in the archive, then it is directly included in the archive.
- If the new solution is neither dominated nor dominates the current solution but it is dominated by at least one solution in the archive, then the decision whether its neighbourhood is explored depends on the acceptance probability.
- If the new solution is neither dominated nor dominates the current solution but it dominates at least one solution in the archive, then it is directly included in the archive.
- If the new solution dominates the current solution and it is not dominated by any solution in the archive, then it replaces directly the current solution in the archive.
- If the new solution dominates the current solution and it is dominated by at least one solution in the archive, then the decision whether its neighbourhood is explored depends on the acceptance probability.

Therefore, for a given temperature level the archive may include dominated solutions, *vis-à-vis* other solutions in the archive. The aim is to allow temporarily dominated solutions in order to enable escaping from local non-dominated fronts. For each temperature level a given number of iterations is performed to foster a more effective local search. Before decreasing the temperature the archive is filtered and non-dominated solutions only are retained for the neighbourhood sampling, as described above, at a lower temperature.

The consideration of the multiple objective function performances is a critical issue to establish the acceptance probability function in multi-objective simulated annealing approaches. Distinct acceptance probability functions have been tested: scalar linear, Chebycheff (strong), weak rules (see also Kubotani and Yoshimura, 2003; Suman and Kumar, 2006), and logistic curve. The difference of performance between the competing solutions is a weighted sum of the

difference of the normalized objective function values. This aggregation takes into account the ranges of values that each objective function attains in the non-dominated frontier computed so far (for normalization purposes, thus avoiding the undesirable effects of aggregating objectives functions expressed in different orders of magnitude).

The difference of performance between the competing solutions *s'* and *s* in objective function j is given by:

$$\delta_j = f_j(s') - f_j(s) \qquad j = 1,...,p \tag{1}$$

The aggregation of these differences is made by a weighted-sum:

$\Delta = \sum_{j=1}^{p} w_j \, \delta_j$, in which w_j is the "weight" assigned to the objective function $f_j(\underline{x})$.

The acceptance probability according to the distinct rules is given by

$$\text{Logistic curve:} \quad P = \frac{2}{1 + e^{\frac{\Delta}{T_k}}} \tag{2}$$

$$\text{Scalar Linear:} \quad P = \min\left(1,\ e^{\frac{-\Delta}{T_k}}\right) \tag{3}$$

$$\text{Chebyshev (Strong):} \quad P = \min\left[1,\ \min_j\left(1,\ e^{\frac{-w_j \, \delta_j}{T_k}}\right)\right] \tag{4}$$

$$\text{Weak:} \quad P = \min\left[1,\ \max_j\left(e^{\frac{-w_j \, \delta_j}{T_k}}\right)\right], \tag{5}$$

in which T_k is the temperature at iteration *k*.

According to the computational experiments carried out in order to select the most favourable acceptance probability function, the weak rule exhibits a large range of acceptance thus imposing a high computational time, although being able to obtain good results. At the other extreme is the Chebyshev (strong) rule that imposes a lower computational burden due to its large range of rejection, but leads in general to a lower number of non-dominated solutions and worst values for the objective functions. The other rules, logistic curve and scalar linear, also lead to good results but the logistic curve has a better computational time on average. Therefore, the acceptance probability function used in the case study is based on the logistic curve. The computational results of this phase of tuning the acceptance probability function (APF) in this multi-objective setting are reported in Appendix B.

The procedure stops when the final temperature specified is attained.

The pseudo-code of this multi-objective simulated annealing approach is presented below.

```
begin
    Create the set of initial random solutions, S_IRS;
    Determine the set of non-dominated solutions, S_NDS;
    for k = 1 to Max_iterations do
        T := Tmax;
        while T>Tmin do
            for i = 1 to size(S_NDS) do
                Pick a solution s=S_NDS(i) from S_NDS
                repeat
                    Select a solution s' in the neighbourhood of solution s;
                    if s' is not dominated by s then
                        if s' is not dominated by any solution in S_NDS then
                            if s' dominates S_NDS(i) then
                                    s' replaces solution i in S_NDS
                            else
                                    s' is included in S_NDS
                            end if
                        else if (rand ∈ [0,1] < APF (s, s', T)) then s ← s';
                        else s' is discarded;
                        end if
                    else if (rand ∈ [0,1] < APF (s, s', T)) then s ← s';
                    else s' is discarded;
                    end if
                until s' have been discarded or included in S_NDS ;
            end for
            T:= cooling_coefficient×T;
        end while
        Update the set of non-dominated solutions, S_NDS;
    end for
end
```

4. Case Study and Illustrative Results

The proposed methodology has been applied to an actual Portuguese radial distribution system with 94 nodes, with some difficult features due to its extension in a rural (sparse) region and poor voltage profile. The network layout is displayed in Figure 5, and its physical characteristics are summarized in Table 2. Full details about the network are available in Pires *et al.* (2009).

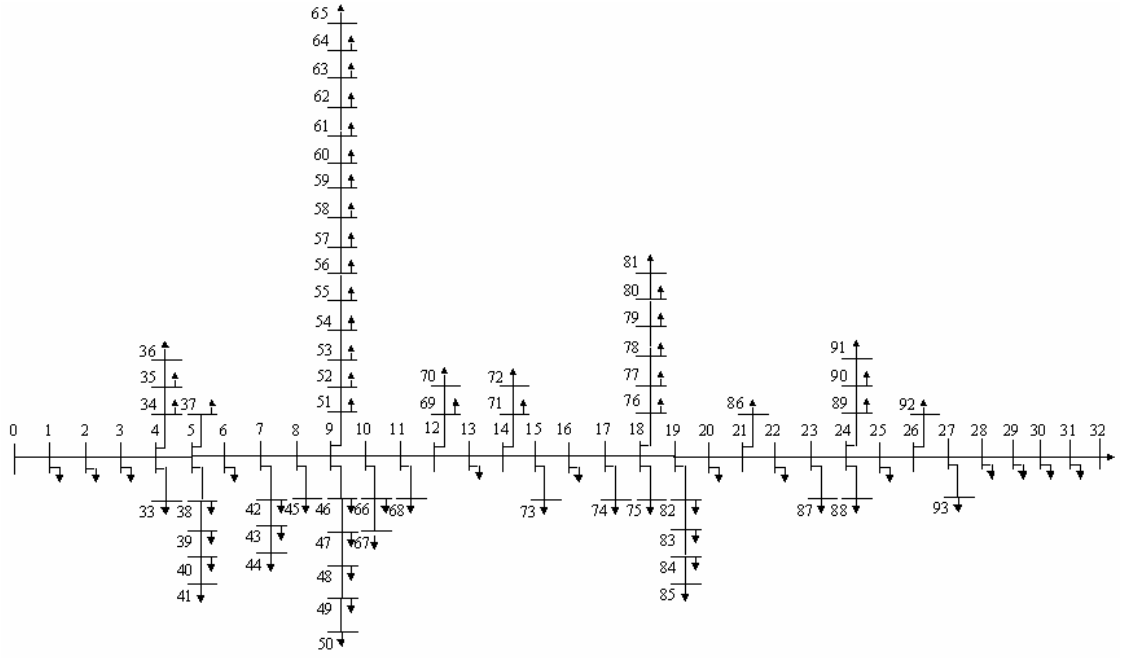

Fig. 5 - Actual radial electrical distribution network with 94 nodes

Table 2 - Network Characteristics

	Minimum	Maximum	Average	St. Dev.
Line length (m)	256	4027	856	559.6
Resistance (Ω/Km)	0.213	1.5	0.745	0.393
Inductance (Ω/Km)	0.356	0.395	0.379	0.011

The capacitors are characterized by their capacity and the acquisition cost (Table 3 - from catalogue prices of a supplier). The study is done for peak load conditions, in which the active power losses are 320.44 kW and the number of nodes not respecting the voltage lower bounds is 39 (in 94 nodes). That is, the network is not working according to regulations in peak load conditions and therefore capacitors must be installed (the zero cost solution is not feasible) for reactive power compensation and voltage profile improvement purposes.

Table 3 - Capacitor dimension and acquisition costs

	Maximum capacity (kVAr)	Cost (Euros)
C1	50	2035
C2	100	2903
C3	140	4545
C4	200	4875
C5	240	5716
C6	300	6578
C7	360	7337
C8	400	9395

Parameters have been tuned through experimentation and the following values were adopted. Temperature is decreased in each step by a factor 0.8. The initial temperature is 1 and the final temperature is 0.0001. The process is repeated 10 times using the information obtained in the previous search.

Figure 6 shows the results obtained with the multi-objective simulated annealing approach described in section 3. The results obtained for this network, operating under the same conditions, with the NSGA II algorithm approach, in which crossover and mutation probabilities have been properly tuned, are also presented for comparison purposes. Both algorithms start with the same set of random initial solutions for the sake of comparison.

The non-dominated frontier is well defined and the solutions are spread all over it. The simulated annealing approach enables the computation of a diverse front, namely regarding the extension towards extreme solutions, that is, in the regions where the cost and the resistive losses objective functions attain their best (minimum) values. In the region with more balanced solutions (the knee of the front) this approach also determined a well-distributed set of solutions organized in a “staircase” structure. The steps are due to the installation of more capacitors while the smooth slope within each step is due to the change of the type of capacitor.

Table 5 presents the objective function values for a representative sample of non-dominated solutions with different characteristics.

Each point displayed in Figure 6 corresponds to a physical compensation scheme (decision variable space). A set of well-dispersed solutions is given in Table 4 leading to resistive power losses and cost given in Table 5 (objective function space). For instance, for solution 1, a capacitor of type 5 is located in node 3, of type 3 in node 4, etc. Solutions 1 and 10 are the extreme solutions, which optimize individually the active power losses and the cost objective functions, respectively.

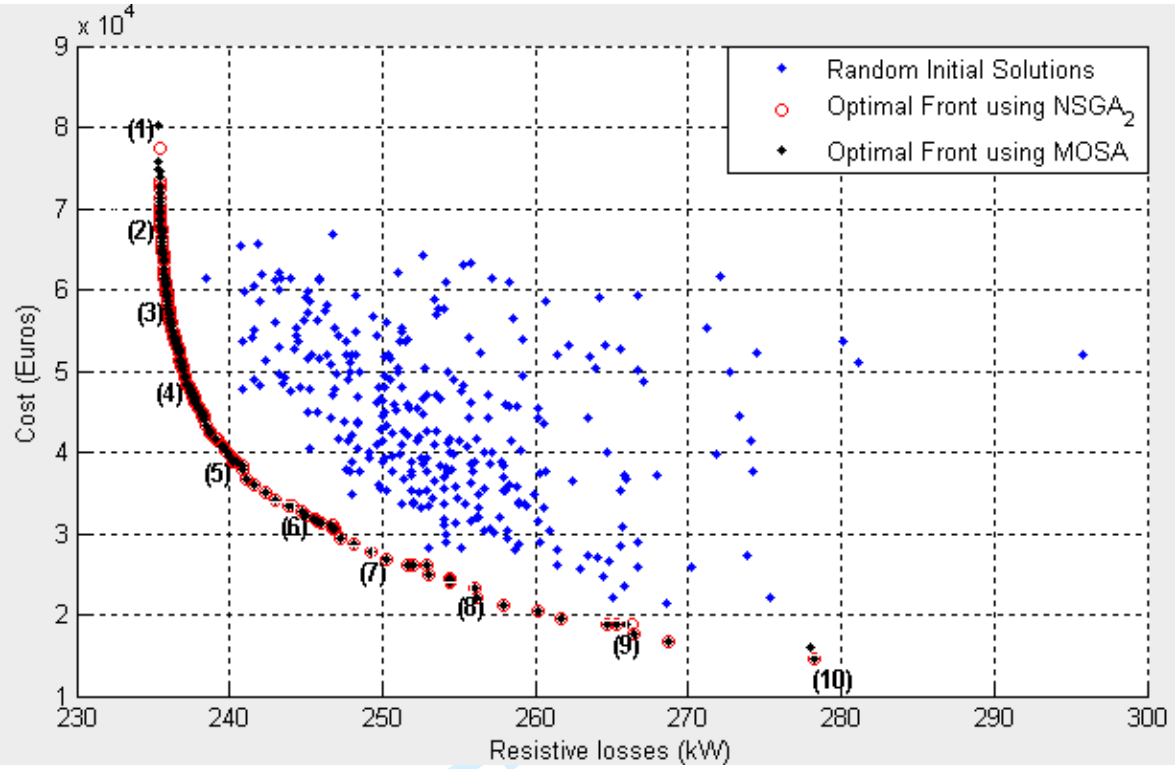

Fig. 6 - Non-dominated front obtained with the multi-objective simulated annealing approach compared with the front computed using NSGA II

Table 4 - Compensation configurations

Solution	Compensation scheme (capacitor installed in each node)	# capacitors
1	0053007000000600000400000000200000100030001002 0200040000740000010000000000000200050011001000	20
2	0000007000000400000000200300010000400000200000 4 0000400040700000020000000100040000006000000000	15
3	0000007000000700000000000400000000000000200000 4 0000000600700000020000000000400000060000000001	11
4	0000000000000700000000005000000000000002000007 0000000070070000000000000000000020000700000000000	8
5	0000000000000700000007000000000000000000000000 0200000070070000000000000000000000070000000000	6
6	0000000000000700000007000000000000000000000000 0000000007000000200000000000000000070000000000	5
7	0000000000000000700000005000000000000000000000 0000000000070000000000000000000000070000000000	4
8	0000000000000000000007000000000000000000000000 0000000000070000000000000000000000070000000000	3
9	0000000000000000000000005000000000000000000000 0000000000000000000000000000005000000700000000000	3
10	0000000000000000000000000007000000000000000000 0000000000000000000000000000000000000000700000	2

Table 5 - Sample of non-dominated solutions (solution id. refers to Figure 6)

Solution	Resistive Losses (kW)	Cost (€)
1	**235.371**	80221
2	235.515	67826
3	236.019	57633
4	237.250	48207
5	239.996	39588
6	244.948	32251
7	249.288	27727
8	256.095	22011
9	265.276	18769
10	278.278	**14674**

These results have been obtained with 10 simulations. The rate of success of each neighbourhood structure is reported in Table 6.

Table 6 – Percentage of success of each neighbourhood structures

Neighbourhood Structure	Average feasible solutions	Average # solutions directly included in the archive	Average # solutions directly replacing other solutions in the archive
(a)	10.9095	2.395	2.719
(b)	10.8677	5.623	21.372
(c)	11.3256	1.218	18.516
(d)	10.3408	1.337	12.746
(e)	11.3270	0.446	6.336
(f)	11.2471	44.103	1.936
(g)	11.3344	34.619	1.369
(h)	22.6478	10.26	35.005

Note: Structures (a-h) refer to the example in Figure 4 (a-h).

The voltage profiles at each node before and after the optimization with the multi-objective simulated annealing procedure, as well as results under different network operating conditions and CPU running times are reported in Appendix C.

Even though it cannot perform actual work, reactive power is required to form the magnetic field in motors and other electric equipment. Therefore, reactive power should be supplied locally to decrease the loading of lines and transmission system losses as well as to improve the voltage profile and steady-state and dynamic stability. A decrease in reactive power causes voltages to fall and a voltage collapse occurs whenever the system is trying to serve much more load than the voltage can support. Shunt capacitors banks adequately sized and located near the loads along the distribution feeders provide several benefits in the exploration of distribution networks, namely in heavy load periods. Shunt capacitors are generally simple devices, in which an insulating dielectric is placed between two metal plates. Capacitors installed in distribution networks may be pole-mounted (least expensive, providing up to 3000 kVAr) or pad-mounted (generally placed underground). These devices may be controlled either locally or centrally by means of communication systems. Automatic capacitor banks consist of steps controlled by a reactive power controller, which ensures that the required reactive power is always connected to the system. The devices may also contribute to improve power quality by providing harmonic filtering.

5. Conclusions

Reactive power compensation is a relevant problem in electrical distribution systems. The adequate sizing and location of capacitors (sources of reactive power that locally supply this demand) contributes to release system capacity and improve voltage level. The case study herein presented is a challenging one because the network is lengthy and is operating in adverse conditions.

A multi-objective simulated annealing approach has been developed, which is specifically designed to provide decision support for planning tasks in this problem. Findings indicate that the simulated annealing approach is able to compute a set of well-distributed and diversified solutions underlying distinct trade-offs between the competing objective functions of economical and technical nature. The thorough characterization of the non-dominated front is valuable information for planning engineers in the selection of satisfactory compromise solutions (compensation schemes) to improve the network operation conditions.

Research is currently underway to design new adequate solution moves and exploit the adaptive behaviour of neighbourhood structures, also for the sake of replicability in other combinatorial problems. Moreover, techniques to provide decision support regarding the selection of a solution for implementation or a set of solutions for further screening are also being developed taking into account the decision maker's preferences.

Acknowledgment

This research has been partially supported by the Portuguese Foundation for Science and Technology under Project Grant PTDC/ENR/64971/2006 "Multi-objective Models in Energy Efficiency Evaluation Problems".

References

C. H. Antunes. C. Barrico. A. Gomes. D. F. Pires and A. G. Martins. "An evolutionary algorithm for reactive power compensation in radial distribution networks", Applied Energy, 86 (7-8), 977-984, 2009.

F. Glover and G. A. Kochenberger (Eds.). Handbook of Metaheuristics, Kluwer Academic Publishers, London, 2003.

H. Kubotani and K. Yoshimura. "Performance evaluation of acceptance probability functions multi-objective SA", Computers & Operations Research, 30 (3), 427-442, 2003.

D. F. Pires, C. H. Antunes and A. G. Martins. "An NSGA-II approach with Local Search for a VAR Planning Multi-Objective Problem", INESC Coimbra Research Report no. 8, 2009. http://www.inescc.pt/documentos/RR8_2009_PiresAntunesMartins.pdf.

B. Suman and P. Kumar. "A survey of simulated annealing as a tool for single and multiobjective optimization". Journal of the Operational Research Society, 57 (10), 1143-1160, 2006.

W. Zhang, F. Li and L. Tolbert. "Review of reactive power planning: objectives, constraints, and algorithms", IEEE Trans. on Power Systems, 22 (4), 2177-2186, 2007.

Appendix A – Multi-objective mathematical model

Figure A.1 illustrates the meaning of the variables and parameters associated with in the electrical network. A feeder is characterized by a resistance, r, and a reactance, x, value (measured in Ohms, Ω), which constitute the characteristic impedance of the power line, $\overline{Z}$.

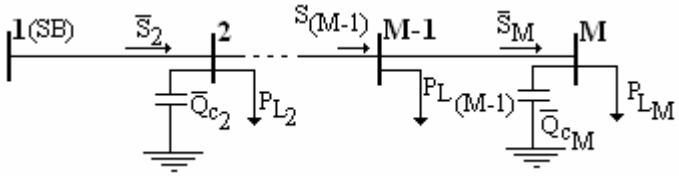

Fig. A.1 - Electrical feeder and corresponding variables

SB – Substation;
k – iteration number;
t – next bus index;
m – previous bus index;
M – number of network buses;
B_m – bus m;
Y – maximum number of capacitors that can be installed;
P_m - active power vector entering bus m;
Q_m - reactive power vector entering bus m;
$\overline{S}_m$ - apparent power vector entering bus m;
Q_{Cm} - reactive compensation installed in bus m;
$\overline{S}_{Cm}$ - apparent compensation power vector installed in bus m;
P_{Lm} - active power demand vector at bus m;
Q_{Lm} - reactive power demand vector at bus m;
$\overline{S}_{Lm}$ - apparent power demand vector at bus m;
$P_{losses(m)}$ - total active power losses vector in all branches subsequent to bus m;
$Q_{losses(m)}$ - total reactive power losses vector in all branches subsequent to bus m;
$\overline{S}_{losses(m)}$ - total apparent power losses vector in all branches subsequent to bus m;
$\overline{V}_m$ - root mean square (rms) voltage vector of bus m;
δ_m –voltage angle in bus m;
$\overline{I}_m$ - current vector that enter bus m;
r_{mt} - resistance of the connection branch from bus m to bus t branch;
x_{mt} - reactance of the connection branch from bus m to bus t branch;
$\overline{Z}_{mt}$ - impedance of the connection branch from bus m to bus t branch;
Q_{Fu} –capacity of capacitor of type u;
C_u – cost of capacitor of type u;
$\overline{X}^*$ - conjugate vector of a generic vector $\overline{X}$.

d_m – real part of voltage vector.
e_m – imaginary part of voltage vector.
a_m^u - binary decision variable denoting whether or not a capacitor of type u is installed in B_m
b_m – coefficient denoting whether or not it is technically possible to install a capacitor in B_m

The vectors structure is described in equations (A.1) to (A.6):

$$\overline{Z}_{mt} = r_{mt} + jx_{mt} \tag{A.1}$$

$$\overline{S}_m = P_m + jQ_m \tag{A.2}$$

$$\overline{V}_m = d_m + je_m \tag{A.3}$$

$$\overline{S}_{Lm} = P_{Lm} + jQ_{Lm} \tag{A.4}$$

$$\overline{S}_{Cm} = -jQ_{Cm} \tag{A.5}$$

$$\overline{S}_{losses(m)} = P_{losses(m)} + jQ_{losses(m)} \tag{A.6}$$

The apparent power equation at bus m is written as

$$\overline{S}_m = \sum_{i=0}^{n} \overline{S}_{t+i} + \sum_{i=0}^{n} \left(\overline{V}_{m(t+i)} \times \left(\frac{\overline{S}_{t+i}}{\overline{V}_{t+i}} \right)^* \right) + \overline{S}_{Lm} + \overline{S}_{Cm} \tag{A.7}$$

Active and reactive powers can be obtained by calculating the real and imaginary parts of $\overline{S}_m$ respectively, (A.8) and (A.9)

$$\overline{P}_m = \mathrm{Re}(\overline{S}_m) \tag{A.8}$$

$$\overline{Q}_m = \mathrm{Im}(\overline{S}_m) \tag{A.9}$$

Apparent power is computed from the last bus of the branch to the first bus, and voltages are computed from the first bus to the last one of the network. The new power values calculated are immediately used in their predecessors' equations and the new voltage values calculated are immediately used in their successors' equations.
The objective functions are the minimization of the system resistive losses (A.10) and the capacitor installation cost (A.11):

$$\text{Min} \sum_{m=1}^{M} \left\{ \text{Re} \left[\sum_{i=0}^{n} \left(\overline{V}_{m(t+i)} \times \left(\frac{\overline{S}_{t+i}}{\overline{V}_{t+i}} \right)^{*} \right) \right] \right\} \quad \text{(A.10)}$$

The index t denotes the identification of the first bus of the lateral.

$$\text{Min} \sum_{m=0}^{M} \sum_{u=1}^{Y} a_m^u c_j \quad \text{(A.11)}$$

$$a_m^u = \begin{cases} 1 & \text{if the new capacitor } Q_{Fu} \text{ is installed in } B_m \\ 0 & \text{otherwise} \end{cases} \quad \text{(A.12)}$$

$$b_m = \begin{cases} 1 & \text{if it is possible to locate a capacitor at } B_m \\ 0 & \text{otherwise} \end{cases} \quad \text{(A.13)}$$

The coefficients b_m represent the technical feasibility of installing capacitors at B_m.

$$Q_{C\,m} = b_m \sum_{u=1}^{Y} a_m^u Q_{Fu} \quad \forall\, m \quad \text{(A.14)}$$

$$\sum_{u=1}^{Y} a_m^u = 1, \forall m \quad \text{(A.15)}$$

The upper and lower bounds for the nodes voltage magnitude is given in (A.16).

$$\overline{V}_{\min} \le \overline{V}_m \le \overline{V}_{\max} \qquad \forall\, m \quad \text{(A.16)}$$

This model is nonlinear and contains both discrete and continuous variables.

Appendix B - Selection of the acceptance probability function

This appendix reports some results of the computational experiments carried out in the phase of tuning the acceptance probability function for the multi-objective problem. Considering the same initial solutions and the same input parameters, the results of each acceptance probability function (10 simulations) are presented in Figure B.1 and Table B.1. The results obtained for each acceptance probability function are similar. The weak rule tends to generate solutions closer to the individual optima of each objective function, and the scalar linear rule gives mostly origin to solutions closer to the best values of the resistive losses objective function. In general, the logistic curve rule and the Chebycheff rule produce solutions well spread in the non-dominated front.

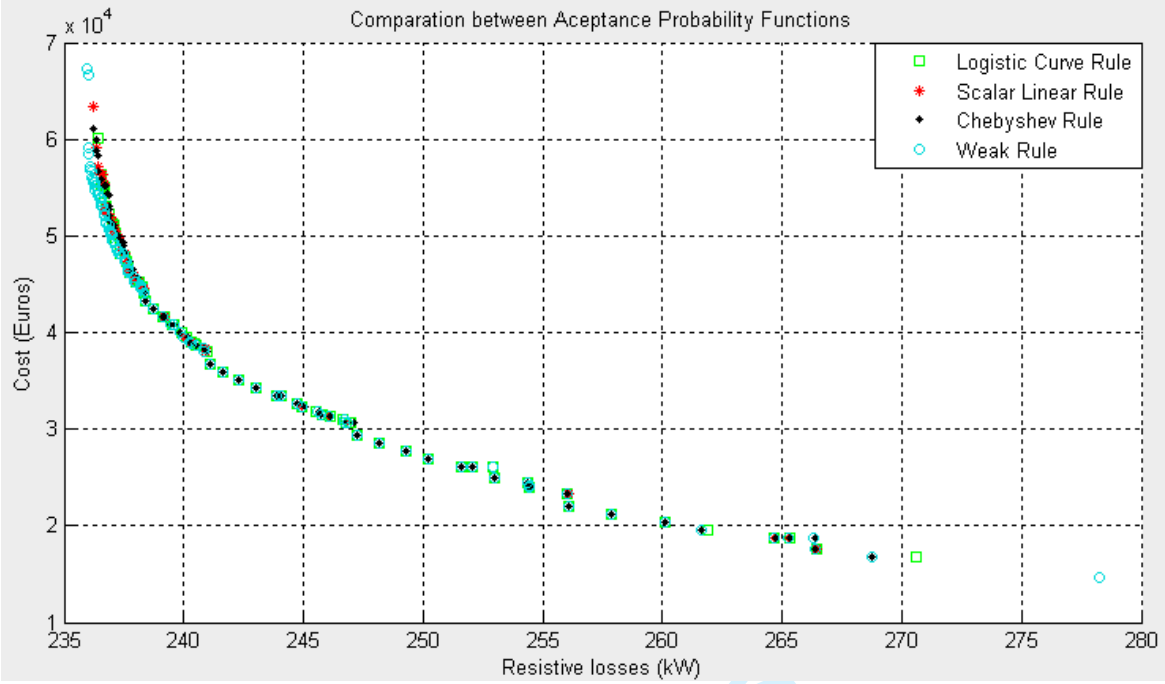

Fig. B.1 - Comparison between the non-dominated fronts of all simulations for each acceptance probability function

Table B.1 – Comparison between the non-dominated fronts (NDF) for each acceptance probability function

Probability functions	# NDF	Minimum Losses	Minimum Cost	Largest consecutive #acceptances	Acceptation vs. Rejection	Time (s)
Logistic Curve Rule	64.5	236.662	17114.1	49.9	50.66% vs. 49.34%	13.081
Scalar Linear Rule	63.9	236.527	17229.5	50.2	51.25% vs. 48.75	13.991
Chebyshev Rule	58.8	236.734	17641.8	3.6	4.87% vs. 95.13%	7.0744
Weak Rule	78.2	236.163	15208.6	167.5	92.44% vs. 7.56%	77.6

Note: These values are 10 simulations averages for each probability function.

Appendix C - Voltage profiles, network operating conditions and CPU times.

Voltage profiles

The study has been carried out for peak load conditions. The active power losses are 320.44 kW. The number of nodes not satisfying the voltage lower bounds is 39 (in 94 nodes; nodes 16-33 and 74-94), with a minimum 0.8697 (in p.u., that is, with respect to the sub-station SE in which V= 15.75 kV) in node 33 (see Fig. 5). The voltage profiles after optimization respect the lower bounds, with a minimum ranging between 0.9004 in node 94 for solution 10 (the individual optimum to the cost objective function) and 0.9268 in node 33 for solution 1 (the individual optimum to the resistive losses objective function).

Results for different network operating conditions

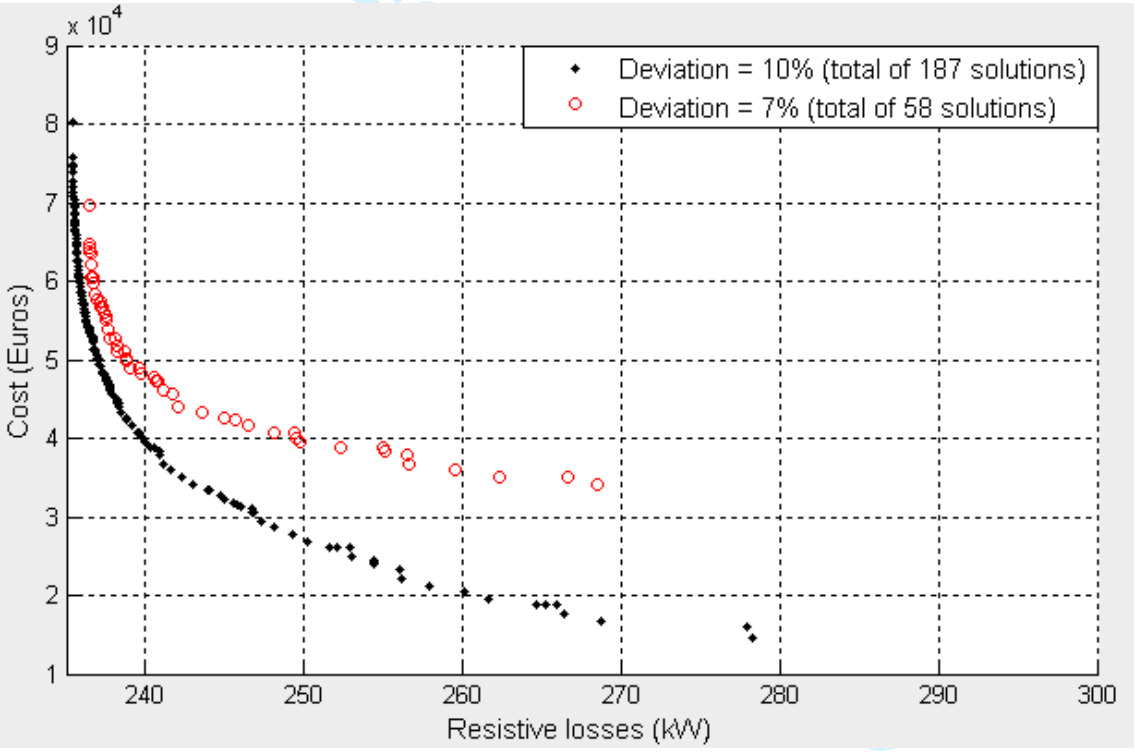

Fig. C.1 - Comparison between non-dominated fronts with 7% and 10% deviation

For the same tuned input parameters, the algorithm presents different results when considering more (1 p.u. ± 7%) or less (1 p.u. ± 10%, according to current regulations in distribution networks) stringent constraints of the maximum voltage amplitude deviation in nodes. This is mainly due to the adverse conditions in which the network is operating. Solutions obtained with

the 1 p.u. ± 10% constraint become infeasible for 1 p.u. ± 7% and the non-dominated front is not as diverse as in the former case because the scope of solutions become narrower.

CPU time and other computational statistical data

Table C.1 – CPU time for different network operating conditions (7% and 10% deviation), including the time spent in running - and number of calls to - the power flow algorithm (10 runs).

CPU time	1	2	3	4	5	6	7	8	9	10
Deviation=7%										
Total time (s):	385.201	282.744	300.385	337.387	309.612	361.033	367.741	368.348	360.874	368.949
Power Flow time (s):	291.270	217.236	227.182	256.923	233.207	274.203	280.638	277.809	270.200	276.548
Power Flow calls (num):	150616	111558	118800	133271	122926	141310	144920	144434	141851	144121
Power Flow time (%):	75.62	76.83	75.63	76.15	75.32	75.95	76.31	75.42	74.87	74.96
MOSA time (s):	93.931	65.508	73.203	80.464	76.405	86.830	87.103	90.539	90.674	92.401
MOSA time (%):	24.38	23.17	24.37	23.85	24.68	24.05	23.69	24.58	25.13	25.04
Deviation=10%										
Total time (s):	958.00	1005.00	786.00	825.00	976.00	971.00	1028.00	856.00	1040.00	854.00
Power Flow time (s):	313.491	330.702	257.296	270.934	323.386	323.505	339.128	284.459	346.474	280.557
Power Flow calls (num):	590600	616420	501528	520671	598234	598110	625265	537651	631962	536478
Power Flow time (%):	32.72	32.91	32.73	32.84	33.13	33.32	32.99	33.23	33.31	32.85
MOSA time (s):	644.509	674.298	528.704	554.066	652.614	647.495	688.872	571.541	693.526	573.443
MOSA time (%):	67.28	67.09	67.27	67.16	66.87	66.68	67.01	66.77	66.69	67.15

Table C.2 – Minimum, maximum and average CPU time for different network operating conditions (7% and 10% deviation), including the time spent in running - and number of calls to - the power flow algorithm (10 runs).

Deviation=7%	Min.	Max.	Average
Total time (s):	282.744	385.201	344.227
Power Flow time (s):	217.236	291.27	260.522
Power Flow calls (num):	111558	150616	135380.7
Power Flow time (%):	74.87	76.83	75.71
MOSA time (s):	65.508	93.931	83.706
MOSA time (%):	23.17	25.13	24.29
Deviation=10%	Min.	Max.	Average
Total time (s):	786	1040	929.9
Power Flow time (s):	257.296	346.474	306.993
Power Flow calls (num):	501528	631962	575691.9
Power Flow time (%):	32.72	33.32	33.00
MOSA time (s):	528.704	693.526	622.907
MOSA time (%):	66.68	67.28	67.00